sciendo

DOI: 10.2478/cdem-2023-0009 CHEM DIDACT ECOL METROL. 2023;28(1-2):157-170

Anna M. BIAŁOSTOCKA[1*], Marcin KLEKOTKA[2], Urszula KLEKOTKA[3]
Piotr R. ŻABIŃSKI[4] and Beata KALSKA-SZOSTKO[3]

SUBSTRATES WITH DIFFERENT MAGNETIC PROPERTIES VERSUS IRON-NICKEL FILM ELECTRODEPOSITION

Abstract: The hereby work presents the iron-nickel alloys electroplated on the different metallic substrates (aluminium, silver, brass) using galvanostatic deposition, with and without presence of the external magnetic field (EMF). The films were obtained in the same electrochemical bath composition - mixture of iron and nickel sulphates (without presence of additives) in the molar ratio of 2 : 1 (Ni : Fe), the electric current density (50.0 mA/cm^2), and the time (3600 s). The mutual alignment of the electric (E) and magnetic field (B) was changeable - parallel and perpendicular. The source of EMF was a set of two permanent magnets (magnetic field strength ranged from 80 mT to 400 mT). It was analysed the surface microstructure, composition, morphology, thickness and the mechanical properties (roughness, work of adhesion). The surface morphology and the thickness of films were observed by Scanning Electron Microscopy (SEM) and Confocal Laser Scanning Microscopy (CLSM). The elemental composition of all FeNi films was measured using Wavelength Dispersive X-Ray Fluorescence (WDXRF). The crystalographic analysis of the deposits was carried out by X-Ray Diffraction. Depending on the used substrate, modified external magnetic field orientation influenced the tribological and physio-chemical properties of the deposited layers. The diamagnetic substrates and EMF application reduced the FeNi thickness and the average crystallites size, in contrast to the paramagnetic substrate. Parallel EMF increased the value of the tribological parameters for CuZn and Ag but decreased for Al. The content of FeNi structure was rising in the case of diamagnetic substrate and the dependence was opposite on the paramagnetic substrate.

Keywords: electrodeposition, magnetic field, magnetohydrodynamics, substrate, thin films, iron-nickel alloys

Introduction

Electrodeposition, also called electroplating, is a very popular technique that produces dense, uniform, and adherent metals, alloys, and composite materials. During that process, the electrolytic cell consists of two electrodes (anode, cathode), which are sinking in the electrolyte. The electrolyte is the environment where the metal ions (the metal of interest) in the liquid state move and thus form the electric circuit between the electrodes. The electrodeposition of FeNi layers from aqueous solutions consists of various stages,

[1] Faculty of Electrical Engineering, Bialystok University of Technology, ul. Wiejska 45D, 15-351 Białystok, Poland, phone +48 85 746 93 97, fax +48 85 746 94 00, ORCID: 0000-0002-7684-2357
[2] Faculty of Mechanical Engineering, Bialystok University of Technology, ul. Wiejska 45C, 15-351 Białystok, Poland, email: m.klekotka@pb.edu.pl, ORCID: 0000-0002-9751-2939
[3] Faculty of Chemistry, University of Bialystok, ul. K. Ciołkowskiego 1K, 15-245 Białystok, Poland, email: u.klekotka@uwb.edu.pl, kalska@uwb.edu.pl, ORCID: UK 0000-0002-1594-5889, BKS 0000-0002-6353-243X
[4] Faculty of Non-Ferrous Metals, AGH University of Science and Technology in Kraków, al. A. Mickiewicza 30, 30-059 Kraków, Poland, email: zabinski@agh.edu.pl, ORCID: 0000-0002-5085-2645
[*]Corresponding author: a.bialostocka@pb.edu.pl

including the transport of solvated species from the solution to the cathode surface (reduction reaction, formation of nuclei) and the growth of the nuclei (2D or 3D deposits). This could take place as the direct incorporation of ions reduced at the interface of deposit-solution. The second way is the formation of adatoms diffusing along the surface to lattice incorporation sites [1, 2]. The nucleation depends on the time of nuclei born, the available area, the value of density of nuclei or their radii. Therefore, it could be studied as instantaneous or progressive. The instantaneous nucleation mechanism is characterised by a constant number of nuclei growing on their primary positions and not forming new nuclei centers on the bare substrate. The radii of these nuclei are large, so the surface morphology is rougher. During the progressive nucleation, the nuclei grow on various positions and form smaller clusters which result in flatter surface morphology [2-4]. Two theories are detailed in the literature which considers the texture evolution in electrodeposits - the theory of the two-dimensional nucleus and the theory of geometrical selection. The first states that the early nuclei dominates the crystallographic orientation of the layer. The second decides about the outward growth mode, which occurs if the electric or magnetic field lines and the direction of the highest growth rate are the same. The blockade of mentioned growth direction creates the possibility of the lateral growth mode. The texture formation is determined by the energy of the system (surface, grain boundary, volume), mainly by the surface free energy (highest value) and its anisotropy [4, 5]. In most cases of FeNi electrodeposition, the microstructure determines its properties. Scientists have made many attempts to control the mechanism of layer growth. They agree that the kind of mechanism depends on the interaction energy between the substrate and the film atoms. When the energy between deposited atoms and the substrate surface is less than the energy between initial and film atoms, the island mechanism of the film growth is carried out. In the case of an inverse ratio of both energies, we are dealing with a layer-by-layer growth mechanism [6, 5].

The electroplating method has been shown to have disproportion at low production costs, a small amount of energy necessary to carry out the process, and a rapid deposition rate. Many methods apply to thin film preparation, but electrodeposition allows to obtain thin films on various surfaces with varied geometries. The FeNi film design for MEMS devices, MRAM, or the other [7, 8] potential applications (medical therapy, biosensors, etc.) as nanocrystalline materials (with grain sizes less than 10 nm) is still getting significant attention from researchers all over the world. The small grain size materials exhibit improved properties compared to conventional coarse-grained materials. The materials vary in terms of electrical resistivity, specific heat, soft magnetic properties, hardness, toughness, corrosion and wear resistance, and thermal conductivity. The modulation of experimental parameters such as substrate type (magnetic or nonmagnetic layer) and electrochemical parameters (electrolyte concentration, deposition potential and time, pH) allow the preparation of materials with a variety of structural, chemical, and magnetic properties [7, 9-16]. When it comes to the nature of the FeNi alloy, electrodeposition is decisive. This is an anomalous deposition. In this case, the less noble metal is deposited preferentially in comparison with the noble metal (Ni). The iron content in the alloy is higher than it results from the composition of the electrolyte. The mentioned mechanism has been many decades. Many scientists have tried to explain what processes occur in it (competition between $FeOH^+$, $NiOH^+$: suppression, adsorption, inhibition). The electroplating conditions themselves are very important, including physicochemical and electrical parameters. Their proper selection influences the morphology, structure,

composition of the obtained alloy and the nature of the process itself (anomalous to normal co-deposition). During the process as a whole, the action of coupled fields (electric and magnetic) is observed. The magnetochemistry has been popularised. Many scientists (Fahidy, Tacken, Janssen, Aogaki, Coey) then and now, analyse and summarise recent research, which leads to a better understanding of the interaction between external magnetic field (EMF) and electrochemical processes. This offers possibilities for the properties of the obtained layers to tailor and is of great importance for future research. The electric current and self-induced magnetic interaction results in the Lorentz force creation. However, the decisive role in the transport phenomena is played by the magnetohydrodynamic (MHD) effect, which is the interaction of flow and magnetic field - the additional convection which changes the transport of mass. The induced flow of electrolyte can be more effective than mechanical agitation and creates micro-MHD vortices at places with non-uniform current distribution (e.g. at the edge of an electrode). It also influences hydrogen bubbles formation, which are smaller after EMF application, and the produced film is free from defects typical of hydrogen evolution [17, 18]. Researchers investigated how the external magnetic field influences the structure of the electrochemically deposited layers. Aogaki and Morimoto explored the influence of the EMF orientation, Matsushima et al. examined the impact of MHD on the growth rate, and Kwon et al. investigated the effect of anisotropy energy [4, 17]. The processing method of morphology tailoring is presented by the application of a high frequency magnetic field, a DC magnetic field, DC magnetic and electric fields, and a traveling magnetic field. The external magnetic field application could result in the following different phase transformation (recovery, recrystallisation, precipitation, ordering, spinodal decomposition, diffusional or martensitic transformations) affecting the variety of nucleation and growth rate, transformation kinetics, variants, and microstructure of obtained phases [18].

The coatings on the machine's parts are still developing, and their state is getting more important. As a result of various manufacturing methods, different surfaces could be obtained, which reflect a lot of tribological properties (friction, wear, lubrication, etc.) and also shouldn't be neglected [19-21]. The roughness is related to wettability, which was discovered and defined by Wenzel's statement:

$$\cos\theta_m = r \cdot \cos\theta_Y \tag{1}$$

where: θ_m - the measured contact angle, θ_Y - Young's contact angle, r - roughness factor: the ratio between solid-liquid interfacial area and the projected area ($r = 1$ for a smooth surface, > 1 for a rough surface).

The roughness can be improved on the boundary zone of two surfaces instead of changing their geometric dimensions [20]. When two surfaces rub against each other, the peak height (R_{pk}) gets worn away, and valley depth (R_{vk}) is a lubricant tank. It is the easiest way to increase the mechanical system's self-efficiency and reduce friction losses which would be reflected in reducing fuel consumption and green house gas emissions. This was the reason for classifying the surface in terms of this roughness. There are other roughness parameters that give better specification of the surface - the surface texturing design (R_{sk} and R_{ku}). R_{sk} is sensitive to deep valleys or high peaks, and zero reflects in the symmetry of the height distribution. R_{ku} informs on the sharpness density of the profile [19, 20]. The increase in the surface roughness of the coatings results in cracks, chipping, and pitting. The roughness influences the friction and the wear rate more broadly than the coating materials themselves [21, 22]. According to several factors, it is possible to obtain

the actual profile of the sample. The surface roughness R_a is the arithmetical deviation of the roughness profile, which evaluates surface quality, and has been widely applied in many industries [23]. However, the single parameter can't get all the surface information. Therefore, maximum profile peak height (R_p) and maximum profile valley depth (R_v) were used to inform about the distance between the highest and deepest point of the profile and the mean line within the evaluation length. Mentioned values are necessary to define the quality of the new surface and its potential application for the industry. An additional parameter, R_z is calculated by measuring the vertical distance from the highest peak to the lowest valley within five sampling lengths. Extremes have a much more significant influence on the final value of the roughness.

Materials and methods

Material and apparatus

The different combinations in respect of external magnetic field of Fe-Ni film deposited on three substrates (Ag, CuZn, Al) were designed to evaluate their properties [24]. Their composition of the substrates from the manufacturer data are following: Ag (Ag 93 %, Fe 7 %), CuZn (Cu 63 %, Zn 37 %), Al (Al 99 %, trace amounts of Cu, Mg and Si). The electrolyte was prepared from chemicals from Avantor: $FeSO_4 \cdot 7H_2O$, $NiSO_4 \cdot 7H_2O$, and H_3BO_3. Bath composition was as follows: 30 % $NiSO_4 \cdot 7H_2O$, 15 % $FeSO_4 \cdot 7H_2O$, 6.18 mol/dm^3 H_3BO_3, what gives molar ratio Ni:Fe equal 2:1 (without any additives).

The samples were cut using the microtone and placed perpendicularly. Then, the thickness of the cross-sections of the deposited layers and their roughness were observed using LEXT OLS 4000 Confocal Laser Scanning Microscopy (CLSM, Olympus, Tokyo, Japan). The final thickness value is the average of ten cross-section points. The values of the latter parameters (R_{sk}, R_{ku}, R_p, R_z, R_v, R_a) were the result of measurements in three parallel lines marked on the sample surfaces and their subsequent averaging. The tests concerning phase changes and composition of the alloys (spot surface measurement) were made with the use of the wavelength dispersive X-ray fluorescence spectrometer (WDXRF) Rigaku Primini II. The surface morphology was analysed by Scanning Electron Microscopy (SEM) method (INSPEC 60, FEI, USA) with varied magnification [25-27]. X-ray diffraction (XRD) was carried out with a microfocus Mo Kα radiation source (λ = 0.713067 Å) - SuperNova (Agilent Technologies, USA) and provided information about the crystal structure of the source, which was a powdered form of the FeNi alloy. The wettability of the samples was measured using an Ossila Contact Goniometer (Ossila, Sheffield, UK). This measurement permitted to distinguish of material surfaces that are hydrophilic or hydrophobic. Contact angle analyses were determined by the sessile drop technique at room temperature and atmospheric pressure. The volume of the water drop was 5 µL. Five independent measurements for pure water were performed for each sample. The obtained results were averaged to reduce the impact of surface non-uniformity. The results of contact angle measurements analysis also allowed for calculating the work of adhesion of a water drop to the solid surface. For this purpose equation (1) given in the Introduction section was used.

FeNi layers deposition

Substrates (before the process) were electrochemically polished and activated by immersion into a mixture of 70 % perchloric acid and 96 % ethanol in a volume ratio of 25 : 75. The FeNi films were obtained by DC mode electrodeposition process with applied current value 10 mA (current density 50 mA/cm^2). The deposition was conducted for 3600 s time at room temperature (21 ± 1) °C, with and without the external magnetic field (EMF) assistance (Fig. 1a-c). Two factory made NdFeB permanent magnets plates (IBS Magnet, 37.5 cm^3 volume) of about 1 T were placed parallel at a distance of 55 mm (Fig. 1d). The effective magnetic field of the magnets was measured (gauge FH51, Magnet-Physik) to be in the range from 80 mT to 200 mT in the volume of electrodeposition. The Pt plate (0.3 cm^2) was used as the anode (width - 6 mm x height - 5 mm x thickness - 0.5 mm). As the cathode 2 cm^2 proper plates were used (width - 10 mm x height - 20 mm x thickness - 0.25 mm). Electrodes were placed parallel, and the distance between them was constant - 20 mm. The bath volume was 20 mL.

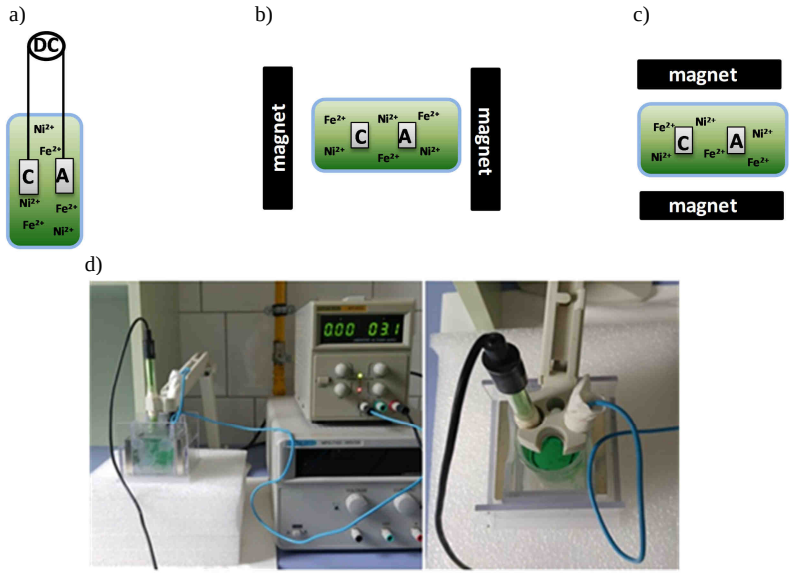

Fig. 1. Schematic presentation of the deposition set-up: a) without the EMF (side view); b) parallel orientation of the EMF - II (top view); c) perpendicular orientation of the EMF - I_ (top view); in respect to the electric field; d) the electrical circuits

Results

Microscopic analysis

SEM images present the morphology of the deposited film, and registered photos are depicted in respective series in Figure 2.

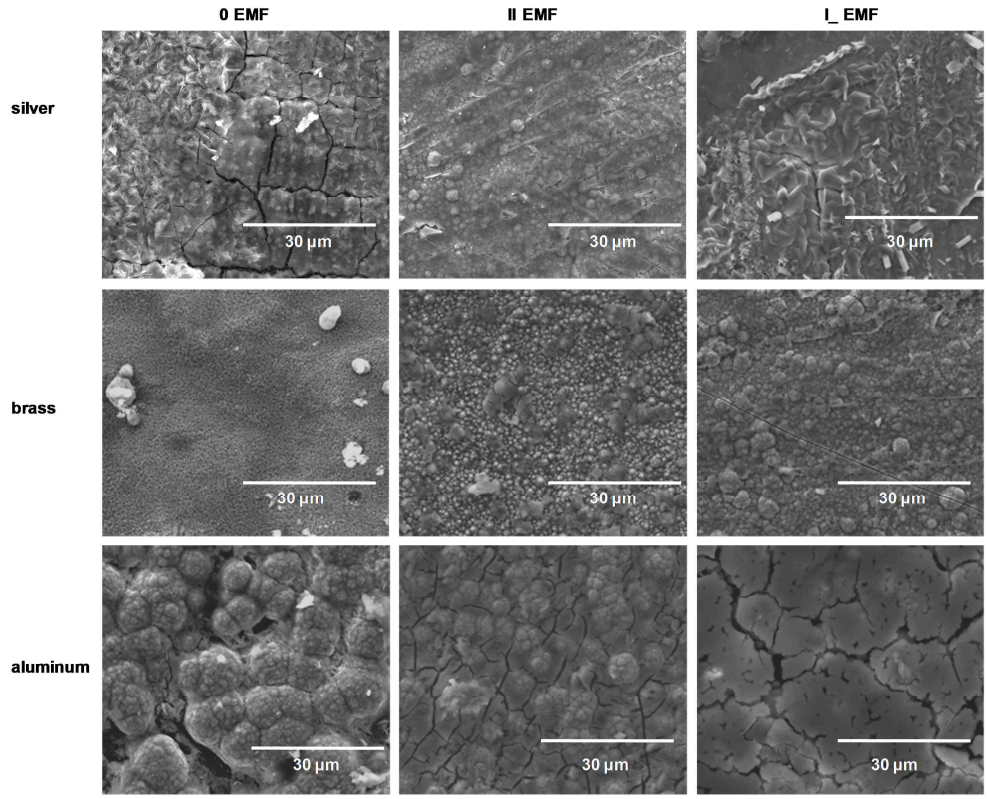

Fig. 2. Set of SEM images of the deposited films with and without EMF (0 EMF): time of deposition - 3600 s; different substrates (silver, brass, aluminium); current density - 50.0 mA/cm^2

Silver - the most uniform (regular, even) polycrystalline thin film is formed when the parallel EMF (II EMF) is applied. The other films (0 EMF, I_ EMF) have very similar topography to each other. For 0 EMF, many small grains can be seen, while for I_ EMF, there are fewer but of bigger sizes.

Brass - the film growth is quite different in comparison to the previous serie. The most even is the film obtained without the EMF application. Only a few large islands are visible here. In the case of II EMF, the film is composed of small seeds with a few bigger ones. For the I_ EMF arrangement, the grains are significantly bigger but in low number. It seems that the nucleation and growth process occurred instantaneously. The nucleated grains are increasing more rapidly than new centres are formed.

Aluminium - the film growth on the aluminium substrate varies significantly between each case of the EMF arrangement. Without the presence of an external magnetic field, the cauliflower forms occurred. In parallel external magnetic field presence, the 3D growth (vertical) is inhibited, and therefore, the 2D (lateral growth) occurs more preferably. Perpendicular external magnetic field application results only in plane growth in the most effective way.

The influence of the external magnetic field orientation and substrate composition is also reflected in film thickness. The results of such investigation are presented in Figure 3a.

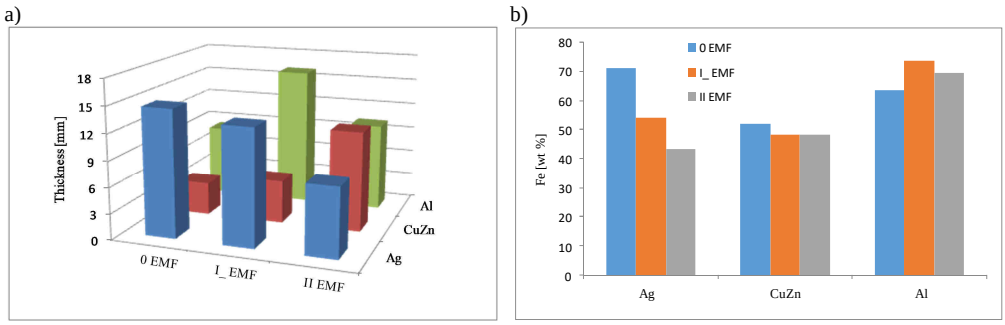

Fig. 3. a) Dependence of the thickness of the FeNi layer obtained on Ag, CuZn, and Al substrates; b) Fe content in the FeNi alloys deposited on three different substrates, current density - 50.0 mA/cm^2

Based on the data presented in Figure 3, a direct relationship was observed between the thickness of the deposited layers and the iron content in the alloys obtained on silver and aluminium substrates. In the case of the brass substrate, no such relation was observed.

The electrodeposition on the diamagnetic substrates (Ag, CuZn) resulted in a decrease of Fe content when the EMF was applied during the deposition process (Fig. 3b), from 71.29 wt. % to 43.53 wt. % for silver, and from 52.13 wt. % to 48.35 wt. % for brass. For Al, the presence of an external magnetic field leads to negative magnetic susceptibility. This can be explained as a result of diamagnetic and paramagnetic substrates, where one reduces and second increases effect of external magnetic field, respectively.

Diffraction measurements

Qualitatively and quantitatively, the quality of the grown layers with respect to crystallinity has been studied on the basis of X-ray diffraction (Fig. 4).

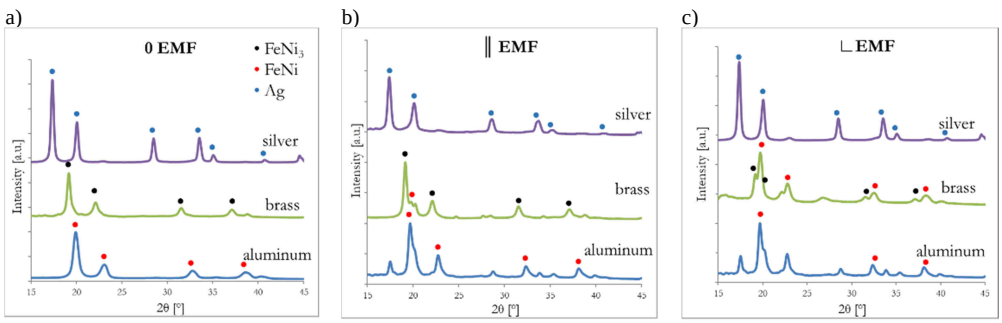

Fig. 4. XRD patterns of films deposited on silver, brass, and aluminium, time 3600 s, current 50.0 mA/cm^2, a) without EMF, b) parallel EMF, c) perpendicular EMF

Quantitative analysis of XRD patterns allows to draw the following conclusions. The values of the crystal cell parameter (*a*) of FeNi or $FeNi_3$ films grown on brass and

aluminium were in the range of 3.55 Å - 3.61 Å and 3.61 Å - 3.72 Å, respectively. These are close to their theoretical values, a = 3.53 Å for FeNi (mp-2213) and a = 3.51 Å for $FeNi_3$ (mp-1418) [25-28]. Regarding crystallite size grown on CuZn and Al, these become largest when electrodeposited without the EMF presence, respectively, d = (22.0 ± 0.5) nm and (13.0 ± 0.5) nm. The EMF presence changed the average size of crystallites and reduced that values to (16.0 ± 0.5) nm and (11.0 ± 0.5) nm, respectively. Scherrer's formula was used to calculate the crystallities values [29]. On the Ag substrate, FeNi film was grown mainly as an amorphous layer due to the absence of typical diffraction peaks for the crystal structure. The external magnetic field application reversed the FeNi and $FeNi_3$ content in the deposited layers (in comparison to the EMF absence). In the case of CuZn substrate, the content of FeNi structure was rising and this dependence was opposite on the Al substrate. Therefore, there is a direct relationship between the crystal structure and the iron content in the alloy. The dominant presence of FeNi in the structure results in an increase of Fe, while $FeNi_3$ - in a decrease. The parallel EMF arrangement suppressed the crystal's nucleation [30]. This dependence is shown in Figure 2.

Based on the analysis of the crystal structure (Fig. 4) of FeNi layers deposited on CuZn and Al substrates, it can be concluded that one of the phases (FeNi or $FeNi_3$) predominates in the absence of EMF. After applying EMF, the situation changes and the involvement of both structures (mixture) is now visible. It is possible to see the trends in the changes in the thickness of the FeNi layers. This is shown in Figure 3a. In an external magnetic field, both structures (FeNi, $FeNi_3$) arrange themselves on the substrate in a heterogeneous manner, which results in a greater thickness of the deposit. Additionally, EMF triggers additional convection and increases mass transport, which is another reason for the effects obtained.

The mutual similarity in terms of the morphology of all the substrates used (Ag, CuZn, Al) simplifies the analysis of the influence of the substrate characteristic on the growth of subsequent layers of the alloy and its final thickness. The conclusions may be similar to those presented above. The insertion of one structure into the substrate results in thinner layers than in the case of two structures present at the same time.

Roughness measurements

The profilograms and 3D surface CLSM images presented in Figure 5 correlate with the results of roughness parameters measurements presented in Figure 6. Especially in the cases of II EMF application on silver and brass substrate, the values of the maximum profile valley depth (R_v) are the highest among the others. The same situation is revealed to the R_p parameter in the aluminium substrate (without EMF). The surfaces of the silver and brass used as the substrates have symmetrical height distribution. The R_a parameter is equal to 0 in the value (Fig. 6). The different value represents the arithmetic mean deviation of the aluminium - three times as large. In the case of diamagnetic substrates, the changes in the R_v values are particularly evident after the parallel EMF application. The largest values of the profile's depth suggest that the FeNi surfaces are relatively depressed. The film on a paramagnetic substrate results in the greatest profile peak height value in the case of electrodeposition without the EMF application. R_p value - 6.57 μm indicates that the FeNi surface contains peaks predominantly. This was confirmed by the appearance of the surface morphology shown in SEM (Fig. 2) - shapes of the cauliflower flower.

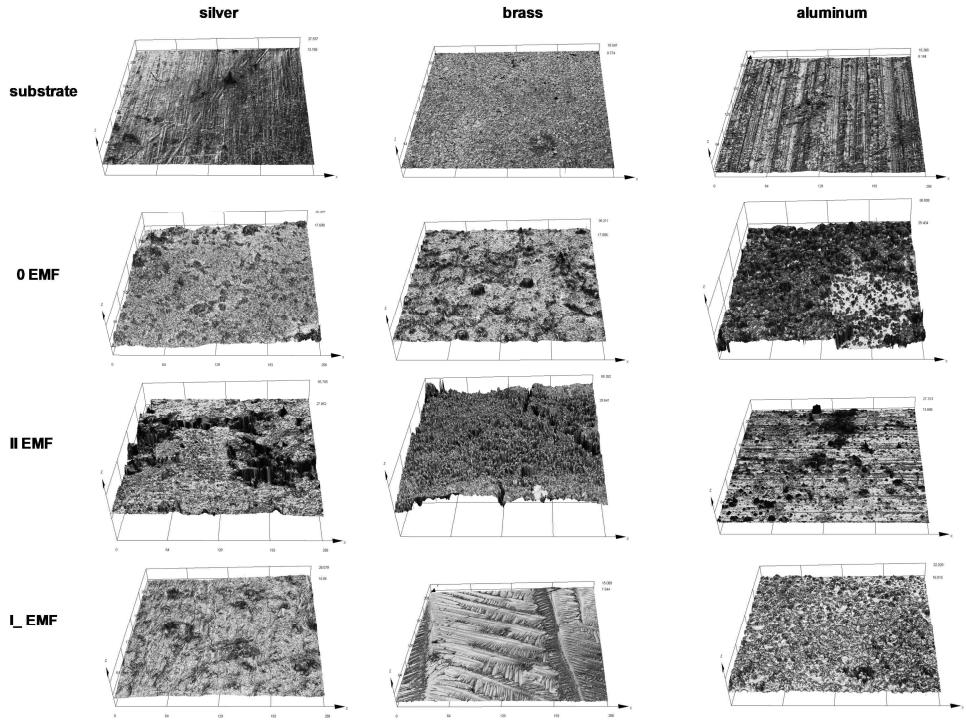

Fig. 5. The 3D surface images on silver, brass, and aluminium substrates

The roughness parameters plotted in Figure 6 are interrelated and inform about the relationship between their value and the EMF arrangement.

The values of all roughness parameters (R_p, R_v, R_z, R_a) change in comparison to clean (polished) substrates. In most cases, application of the I_ EMF resulted in decreased values of mentioned parameters compared to 0 EMF (expect Ag-R_p). The nature of changes was the same for diamagnetic substrates (Ag, CuZn) at both EMF arrangement and without it. The situation changes after using the external magnetic field. However, their values are subject to variability, especially after the II EMF application. The rapid increase in the roughness parameters values of FeNi alloys occurred on diamagnetic and decrease of mentioned parameters obtained on the paramagnetic substrate (Al). An inversely proportional relationship was observed between the FeNi content in the crystal structure of the alloy (Fig. 4) and the values of individual roughness parameters. The II EMF arrangement contributes to increase in R_p, R_v, R_z, R_a but for Al the tendency is already the opposite. The less range of changes between R_p and R_v parameters (Ag, CuZn) in the case 0 EMF allows to conclude that electrodeposited alloy is uniform.

Some investigations have shown that there is a relationship between the thickness of the FeNi film (Fig. 3a) and value of the R_a parameter [5]. The found mechanism is manifested by a directly proportional correlation between them. This takes place only in the case of a brass substrate. The other two cases deviate from this rule. It could be connected with better uniformity of the layer and differences between R_p and R_v when it comes to the value.

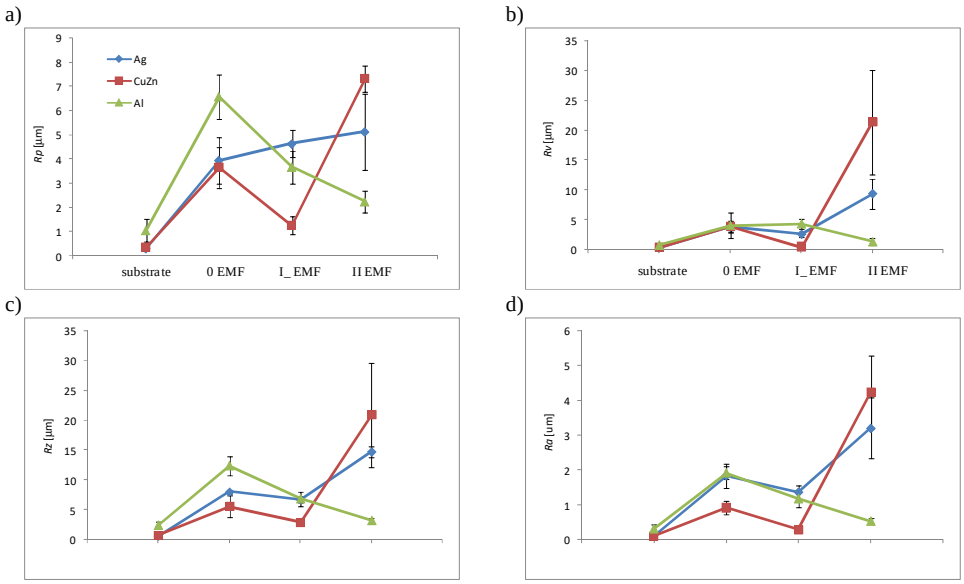

Fig. 6. Comparison of deposited films roughness parameters values on the different substrates (Ag, CuZn, Al): a) R_p, b) R_v, c) R_z, d) R_a

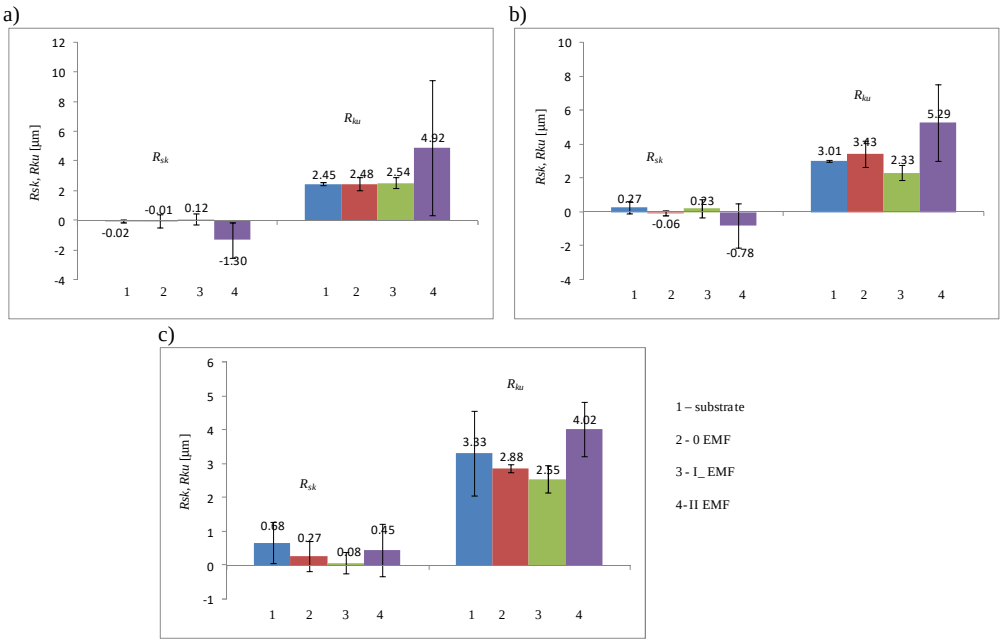

Fig. 7. Surface roughness characteristics, based on the average values of R_{sk} and R_{ku} parameters for substrates: a) Ag, b) CuZn, c) Al, and FeNi layers

In the case of silver and brass substrates, surfaces get more valleys (negative R_{sk}) than aluminium. On the other hand, kurtosis (R_{ku}) characterises the sharpness of the profile. When the R_{ku} value is bigger than 3 μm, the surface gets spiky. This is visible, mainly when II EMF is applied during the deposition process on all substrates. In the other cases, the kurtosis values suggest that height distribution is relatively flat with lots of moderately height protrusions (Fig. 6) [31]. It concerns the negative skewness (R_{sk}) values (Fig. 7): -1.30 μm and -0.78 μm and suggests surfaces with more valleys than peaks. The same is in the case of kurtosis (R_{ku}) values greater than 3 μm (4.92 μm and 5.29 μm). In this situation, the distribution is called leptokurtic [31]. The surfaces are called spiky.

Work of adhesion calculations

The results of work of adhesion calculations (W_{sl}) well explain the microstructure evolution of the FeNi films on the different substrates (Fig. 8). When the specific surface energy (SSE) of the substrates is less than the SSE of the films, the crystals form conglomerates and film gets rougher with high thickness heterogeneity [5, 6]. The Volmer-Weber deposition mechanism occurs, called island (volume) growth [5]. All of the above is confirmed by the obtained values of R_{sk} and R_{ku} (Fig. 7). These is coherent with morphologies presented in Figure 2. Large variations in surface morphology show the layers deposited on silver or brass (II EMF) and aluminium (0 EMF) substrate. Moreover, in the case of all layers, it can be noticed that if the values of R_a parameters are lower, their work of adhesion is greater (Fig. 8). This means that in these cases, the wettability of smoother coatings is higher.

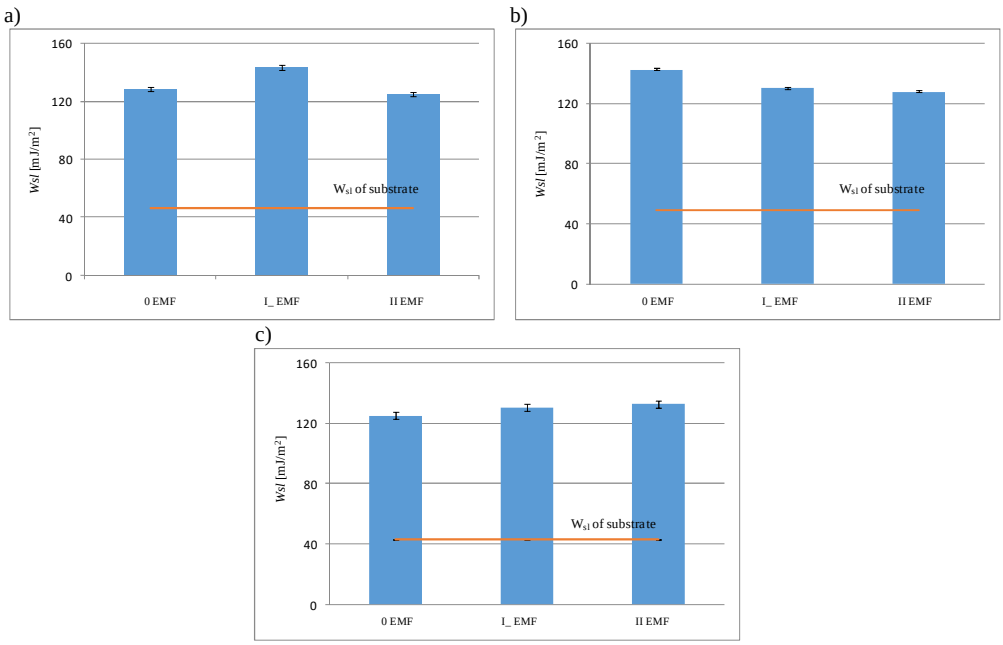

Fig. 8. Values of work of adhesion of the FeNi films on substrates: a) silver, b) brass, c) aluminium, and the substrates itself

Discussion

The influence of the external magnetic field (II EMF or I_ EMF) on film growth is clearly seen in the set of SEM images (Fig. 2). On the silver and brass substrate, II EMF application caused 2D growth (small grains) of the FeNi alloys and I_ EMF - 3D (bigger ones). The parallel and perpendicular setting of the external magnetic field orientation results the revealed growth mode (lateral versus vertical). In the case of aluminium substrate, the evident impact of MHD flow gives rise to micro-MHD flows. In both EMF arrangements (II and I_), 2D growth is observed. The above statements are confirmed by the sizes of the crystal lattice parameters - decrease in the size of the crystallites. The magnetic properties of the substrates affect both the thickness of the deposited layer and the iron content. In the case of crystal structures obtained on CuZn and Al substrates (not amorphous on Ag substrate), the external magnetic field affects the layer thickness, increasing it only in the presence of more than one structure in the alloy composition (FeNi or $FeNi_3$). The EMF application influences all of the roughness parameters which is correlated with the MHD effect. The values of the roughness parameters (R_{sk} and R_{ku}) confirm the layer growth mechanism present in these cases. The magnetic properties of the substrates have a visible impact on the composition of the deposited FeNi alloys. Diamagnetic reduce and paramagnetic increase the iron content, which is directly related to their magnetic susceptibility.

Conclusion

Surface roughness is a very important aspect of the manufacturing process, but it is often overlooked. By changing the substrate (see: its magnetic properties), an alloy with the intended composition can be obtained, knowing that diamagnetic decreases and paramagnetic increases the Fe content in the film. This is directly reflected in its crystal structure (FeNi or $FeNi_3$) - an external magnetic field results in a reduction in the size of the crystallites, which was demonstrated during the analysis of the performed data. Applied substrates varied in terms of their cell parameter: CuZn - 3.62 Å - 3.69 Å, Ag - 4.08 Å, Al - 2.86 Å, which affected the growth regime itself and the form of deposited layer. The arrangement of the parallel (II) or perpendicular (I_) orientation of the EMF, as well as type of the substrate, results in various values of roughness parameters which impact the alloys' physiochemical properties. This is particularly important in the case of mutual parallel alignment of the electric and magnetic fields - diamagnetic substrates increase and paramagnetic substrates decrease the roughness values. All information relating to the roughness (R_{sk}, R_{ku}, R_p, R_v, R_z, R_a) of the obtained surfaces, i.e. 2D increase (II EMF) and 3D increase (I_ EMF), can significantly accelerate the application of a given alloy on a selected substrate and thus saves time.

Competition between energies (substrate and layer) determines the film growth mechanism (layered or grain growth) and morphology evolution (roughness). All of the obtained films are hydrophilic. The test results obtained in this work have both scientific and utilitarian significance, especially that a better understanding of the dependencies mentioned above gives the opportunity to form layers for specific industrial applications.

Acknowledgements

This work was partially financed by the EU fund as part of the projects: POPW.01.03.00-20.034/09 and POPW.01.03.00-20-004/11. This research was realised in the frame of work No. WZ/WE-IA/7/2023 and WI\WM-IIB\3\2023, which were partially financed from research funds of the Ministry of Education and Science Poland.

References

[1] Hwang BJ, Santhanam R, Lin YL. Nucleation and growth mechanism of electroformation of polypyrrole on a heat-treated gold/highly oriented pyrolytic graphite. Electrochim Acta. 2001;46:2843-53. DOI: 10.1016/S0013-4686(01)00495-9.

[2] Kołodziejczyk K, Miękoś E, Zieliński M, Jaksender M, Szczukocki D, Czarny K, et al. Influence of constant magnetic field on electrodeposition of metals, alloys, conductive polymers, and organic reactions. J Solid State Electrochem. 2018;22:1629-47. DOI: 10.1007/s10008-017-3875-x.

[3] Palomar-Pardave M, Scharifker BR, Arce EM, Romero-Romo M. Nucleation and diffusion-controlled growth of electroactive centers reduction of protons during cobalt electrodeposition. Electrochim Acta. 2005;50:4736-45. DOI: 10.1016/j.electacta.2005.03.004.

[4] Krause A, Uhlemann M, Gebert A, Schultz L. A study of nucleation, growth, texture and phase formation of electrodeposited cobalt layers and the influence of magnetic fields. Thin Solid Films. 2006;1694-700. DOI: 10.1016/j.tsf.2006.06.003.

[5] Zubar TI, Sharko SA, Tishkevich DI, Kovaleva NN, Vinnik DA, Gudkova SA, et al. Anomalies in Ni-Fe nanogranular films growth. Alloy Compd. 2018;20:2306-15. DOI: 10.1016/j.jallcom.2018.03.245.

[6] Zubar TI, Fedosyuk VM, Trukhanov SV, Tishkevich DI, Michels D, Lyakhov D, et al. Method of surface energy investigation by lateral AFM: application to control growth mechanism of nanustructured NiFe films. Sci Rep-UK. 2020;10:14411. DOI: 10.1038/s41598-020-71416-w.

[7] Dragos O, Chiriac H, Lupu N, Grigoras M, Tabakovic I. Anomalous codeposition of fcc NiFe nanowires with 5-55% Fe and their morphology, crystal structure and magnetic properties. J Electrochem Soc. 2016;163:D83-94. DOI: 10.1149/2.0771603jes.

[8] Ohba M, Scarazzato T, Espinosa DCR, Panossian Z. Study of metal electrodeposition by means of simulated and experimental polarization curves: Zinc deposition on steel electrodes. Electrochim Acta. 2019;309:86-103. DOI: 10.1016/j.electacta.2019.04.074.

[9] Kuru H, Colak Aytekin N, Köckar H, Haciismailoğlu M, Alper M. Effect of NiFe layer thickness on properties of NiFe/Cu superlattices electrodeposited on titanium substrate. J Mater Sci-Mater EL. 2019;30:17879-89. DOI: 10.1007/s10854-019-02140-z.

[10] Fazli S, Bahrololoom ME. Electrodeposition of nanostructured permalloy and permalloy-magnetite composite coatings and investigation of their magnetic properties. Metall Mater Trans A. 2016;47A. DOI: 10.1007/s11661-016-3575-7.

[11] Gurrappa I, Binder L. Electrodeposition of nanostructured coatings and their characterization - a review. Sci Technol Adv Mater. 2008;9:043001. DOI: 10.1088/1468-6996/9/4/043001.

[12] Tudela I, Zhang Y, Pal M, Kerr I, Mason TJ, Cobley AJ. Ultrasound-assisted electrodeposition of nickel: Effect of ultrasonic power on the characteristics of thin coatings. Surf Coat Technol. 2015;264:49-59. DOI: 10.1016/j.surfcoat.2015.01.020.

[13] Nurjaman SF, Aziz N. Optimization of tin magneto electrodeposition under additive electrolyte influence using Taguchi method application. Mater Sci Forum. 2016;860:85-91. DOI: 10.4028/www.scientific.net/MSF.860.85.

[14] Rousse C, Msellak K, Fricoteaux P, Merienne E, Chopart J-P. Magnetic and electrochemical studies on electrodeposited Ni-Fe alloys. Magnetohydrodynamics. 2006;42:371-8. DOI: 10.22364/mhd.42.4.3

[15] Gong J, Riemer S, Kautzky M, Tabakovic IJ. Composition gradient, structure, stress, roughness and magnetic properties of 5-500 nm thin NiFe films obtained by electrodeposition. Magn Magn Mater. 2016;398:64-9. DOI: 10.1016/j.jmmm.2015.09.036.

[16] Gamburg YD, Zangari G. Theory and Practice of Metal Electrodeposition. New York, Dordrecht, Heidelberg, London: Springer; 2011. ISBN: 9781441996688. DOI: 10.1007/978-1-4419-9669-5.

[17] Monzon LMA, Coey JMD. Magnetic fields in electrochemistry: The Lorentz forces. A mini-review. Electrochem Commun. 2014;42:38-41. DOI: 10.1016/j.elecom.2014.02.006.

[18] Asai S. Recent development and prospect of electromagnetic processing of materials. Sci Technol Adv Materials. 2000;1:191-200. DOI: 10.1016/S1468-6996(00)00016-4.

[19] Sedlaček M, Podgornik B, Vizintin J. Correlation between standard roughness parameters skewness and kurtosis and tribological behaviour of contact surfaces. Tribol Int. 2012;48:102-12. DOI: 10.1016/j.triboint.2011.11.008.
[20] Sedlaček M, Gregorčič P, Podgornik B. Use of the roughness parameters Ssk and Sku to control friction - a method for designing surface texturing. Tribol Trans. 2017;60:260-6. DOI: 10.1080/10402004.2016.1159358.
[21] Svahn F, Kassman-Rudolphi A, Wallen E. The influence of surface roughness on friction and wear of machine element coatings. Wear. 2003;254:1092-8. DOI: 10.1016/S0043-1648(03)00341-7.
[22] Jiang J, Arnell RD. The effect of substrate surface roughness on the wear of DLC coatings. Wear. 2000;239:1-9. DOI: 10.1016/S0043-1648(99)00351-8.
[23] Yang D, Wang Q, Tang J, Xia F, Zhou W, Wen Y. Correlation analysis of roughness surface height distribution parameters and maximum mises stress. Surf. Topogr.: Metrol Prop. 2021;10:015046. DOI: 10.1088/2051-672X/ac5d6b.
[24] Okamoto N, Wang F, Watanabe T. Adhesion of electrodeposited copper, nickel and silver films on copper, nickel and silver substrates. J Japan Inst Metals Materials. 2004;45:3330-3. DOI: 10.2320/matertrans.45.3330.
[25] Persson K. Materials Data on $FeNi_3$ (SG:221) by Materials Project. 2015. DOI: 10.17188/1190197.
[26] Persson K. Materials Data on FeNi (SG:123) by Materials Project. 2016. DOI: 10.17188/1197364.
[27] Kądziołka-Gaweł M, Zarek M, Popiel E, Chrobak A. The crystal structure and magnetic properties of selected fcc FeNi and $Fe_{40}Ni_{40}B_{20}$ alloys. A. Phys Pol A. 2009;117:412-4. DOI: 10.12693/APhysPolA.117.412.
[28] Trong DN, Long VC. Effects of number of atoms, shell thickness, and temperature on the structure of Fe nanoparticles amorphous by molecular dynamics method. Appl Mech Mater. 2021;6894514:1-12. DOI: 10.1155/2021/9976633.
[29] Bokuniaeva AO, Vorokh AS. Estimation of particle size using the Debye equation and the Scherrer formula for polyphasic TiO_2 powder. J Phys: Conf Ser. 2019;1410:012057. DOI: 10.1088/1742-6596/1410/1/012057.
[30] Białostocka A, Klekotka U, Kalska-Szostko B. Modulation of iron-nickel layers composition by an external magnetic field. Chem Eng Commun. 2020;206:804-14. DOI: 10.1080/00986445.2018.1528239.
[31] Egbu J, Ohodnicki Jr PR, Baltrus JP, Talaat A, Wright RF, McHenry ME. Analysis of surface roughness and oxidation of FeNi-based metal amorphous nanocomposite alloys. J All Com. 2022;912:165155. DOI: 10.1016/j.allcom.2022.165155.